Available online at www.sciencedirect.com
ScienceDirect
European Journal of Medicinal Chemistry 43 (2008) 2373–2379
EUROPEAN JOURNAL OF MEDICINAL CHEMISTRY
http://www.elsevier.com/locate/ejmech

Original article

Lanostane-type triterpenoids from the sclerotia of *Inonotus obliquus* possessing anti-tumor promoting activity

Sayaka Taji [a], Takeshi Yamada [a], Shun-ichi Wada [a], Harukuni Tokuda [b], Kazuo Sakuma [c], Reiko Tanaka [a,*]

[a] *Department of Medicinal Chemistry, Osaka University of Pharmaceutical Sciences, 4-20-1 Nasahara, Takatsuki, Osaka 569-1094, Japan*
[b] *Department of Biochemistry, Kyoto Prefectural University of Medicine, Kamigyo-ku, Kyoto 602-0841, Japan*
[c] *Salad Melon Company Limited, 105 Nitshinn, Nayoro City, Hokkaido 096-0066, Japan*

Received 2 August 2007; received in revised form 12 December 2007; accepted 10 January 2008
Available online 8 February 2008

Abstract

Two new lanostane-type triterpenoids, **1** and **2** besides two known lanostane-type triterpenoids, **3** and **4** were isolated from the sclerotia of *Inonotus obliquus*. Their structures were determined to be lanosta-8,23*E*-diene-3β,22*R*,25-triol (**1**) and lanosta-7:9(11),23*E*-triene-3β,22*R*,25-triol (**2**) by spectral data. These compounds were tested for their anti-tumor-promoting activity using a short-term in vitro assay for EBV–EA activation induced by TPA. Compounds **1**, **2** and **4** were stronger than the positive control, oleanolic acid. The most abundant compound **4** was investigated for the inhibitory effect in a two-stage carcinogenesis test on mouse skin using DMBA as an initiator and TPA as a promoter. Compound **4** was found to exhibit the potent anti-tumor promoting activity in the in vivo carcinogenesis test.

Keywords: Lanosta-8,23*E*-diene-3β,22*R*,25-triol; Lanosta-7:9(11),23*E*-triene-3β,22*R*,25-triol; 3β-Hydroxylanosta-8,24-dien-21-al: EBV–EA activation; Mouse-skin carcinogenesis assay

1. Introduction

In recent years, more effective and safer agents are intensively required for chemoprevention of human cancer, and natural products from plants and their synthetic derivatives are expected to play an important role in developing innovative agents to inhibit the onset of cancer [1,2]. In particular, there is a need for agents targeted at the promoting stage of carcinogenesis in the two or multi-stage theory [3] since it is difficult to avoid unfavorable hits by tumor-initiating agents in human life, but tumor promotion is a long and reversible stage that can be efficiently suppressed [4,5].

Inonotus obliquus (Pers.: Fr.) Pil. [=*Fuscoporia obliqua* (Pers.: Fr.) Aoshima], called kabanoanatake (in Japan) and chaga or tchaga (in Russia), is a white-rot fungus belonging to the family *Hymenochaetaceae Donk* [6], and the distribution of this mushroom is recognized in Europe, Asia, and North America. The imperfect form of *I. obliquus* occurs parasitically on trunks, usually of *Betula* (birch), and more rarely also on *Ulmus*, *Alnus*, and *Fraxinus*. The perfect form with pores and basidia is produced under the bark [7], only after the tree's death. Extractives from the sclerotium of *I. obliquus* have been known to have a positive effect on controlling cancer, human immunodeficiency virus 1 (HIV-1), and digestive disease [8]. Anti-tumor experiments with *n*-hexane extractives of *I. obliquus* have been conducted, and it has been reported that inotodiol has a significant anticancer effect on walker 256 carcinosarcoma and MCF-7 human mammary adenocarcinoma [9]. Recently, we reported structure determination of two new lanostane-type triterpenoids isolated from the sclerotia, inonotsuoxides A and B (22*R*,25-epoxylanost-8-ene-3β,24*S*-diol and 22*S*,25-epoxy epimer), and the results of in

* Corresponding author. Tel./fax: +81 72 690 1084.
E-mail address: tanakar@gly.oups.ac.jp (R. Tanaka).

0223-5234/$ - see front matter © 2008 Elsevier Masson SAS. All rights reserved.
doi:10.1016/j.ejmech.2008.01.037

vivo mouse-skin carcinogenesis test using DMBA/TPA model about inotodiol, the most abundant triterpene of this sclerotia [10].

Careful examination of the sclerotia of *I. obliquus* has led to the isolation of two new lanostane-type triterpenes **1** and **2**, besides two known triterpenes **3** and **4**. The structures of the new compounds **1** and **2** were determined on the basis of spectroscopic data and the known compounds were identified as lanosta-8,24-dien-3β,21-diol (**3**) [11] and 3β-hydroxylanosta-8,24-dien-21-al (**4**) [12] by comparison of their spectral data with those reported in the literature. This report deals with the structure determination of compounds **1** and **2** and results of in vitro and in vivo anti-tumor promoting activity of **1**–**4**. The assay methods employed were an in vitro assay estimating the inhibitory effect on Epstein-Barr virus early antigen (EBV–EA) activation induced by TPA [13] and an in vivo two-stage mouse-skin carcinogenesis assay using DMBA as an initiator and TPA as a promoter [14].

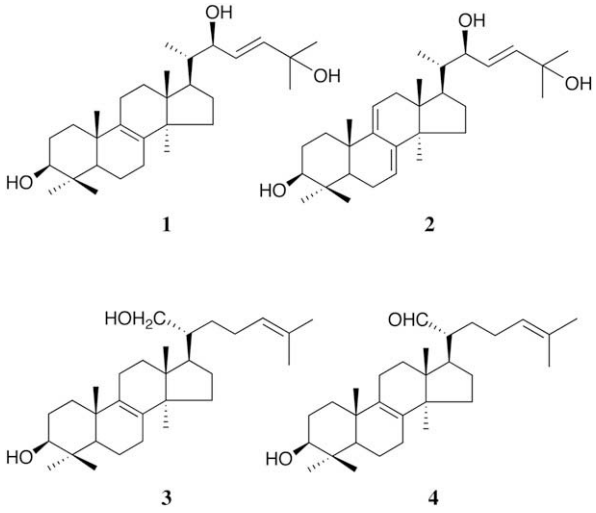

2. Results and discussion

2.1. Chemistry

Sclerotia of *I. obliquus* was extracted with $CHCl_3$, and the extract was separated with silica gel column chromatography, medium-pressure liquid chromatography (MPLC) and high-pressure liquid chromatography (HPLC). Two new (**1**, **2**) and two known (**3**, **4**) triterpenes were obtained. Compounds **3** and **4** were confirmed as lanosta-8,24-dien-3β,21-diol (**3**) [11] and 3β-hydroxylanosta-8,24-dien-21-al (**4**) [12] because their physical and spectral data showed good agreement with those already published.

The molecular formula of compound **1** was assigned as $C_{30}H_{50}O_3$ (M^+; *m/z* 458.3759) by HREIMS. The IR spectrum showed a hydroxyl group (ν_{max} 3447 cm^{-1}). The ^1H and ^{13}C NMR spectra ($CDCl_3$) of **1** (Table 1) exhibited eight tertiary methyl groups, eight methylenes, five sp^3 methines including two oxymethines [δ_H 3.24 (1H, dd, $J = 11.7$, 4.6 Hz); δ_C 79.0 (d)]; [δ_H 4.23 (1H, dd, $J = 7.0$, 3.4 Hz); δ_C 74.5 (d)], a disubstituted double bond [δ_H 5.70 (1H, dd, $J = 16.1$, 7.0 Hz), δ_C 129.4 (d); δ_H 5.78 (1H, d, $J = 16.1$ Hz); δ_C 135.9 (d)], five sp^3 quarternary carbons including one oxycarbon [δ_C 82.0 (s)] and a tetrasubstituted double bond [δ_C 134.1 (s), 134.6 (s)]. The planar structure of **1** was determined by HMBC and ^1H–^1H COSY spectra. The HMBC spectrum of **1** (Table 1) indicated a long-range correlation between Me-18 (δ_H 0.73) and each of C-12, C-13, C-14 and C-17, between Me-19 (δ_H 0.98) and C-1, C-5, C-9 and C-10, between Me-21 (δ_H 0.93, d) and C-17, C-20 and C-22, between Me-26 (δ_H 1.35) and C-24, C-25 and C-27, between Me-27 (δ_H 1.36) and C-24, C-25 and C-26, between Me-28 (δ_H 1.00) and C-3, C-4, C-5 and C-29, between Me-29 (δ_H 0.81) and C-3, C-4, C-5 and C-28, between Me-30 (δ_H 0.83) and C-8, C-13, C-14 and C-15, between H-22 (δ_H 4.23) and C-20, C-21, C-23 and C-24, between H-23 (δ_H 5.70) and C-22 (δ_C 74.5, d), C-24 (δ_C 135.9, d) and C-25 (δ_C 82.0, s), between H-24 (δ_H 5.78) and C-22, C-23 (δ_C 129.4, d), C-25 (δ_C 82.0, s), C-26 (δ_C 24.3, q) and C-27 (δ_C 24.5, q), respectively. In the ^1H–^1H COSY spectrum (Table 1), H-23 correlated with H-22 (δ_H 4.23) and H-24, but H-24 correlated only with H-23. The above spectral data suggested that the structure of **1** was lanosta-8,23-diene-3,22,25-triol. The absolute configuration of **1** at C-20 was established as C-20β because of significant NOEs for Me-18/H-20; Me-18/Me-21; H-20/H-16β. One of the hydroxyl groups was C-3β as shown by the chemical shift and the coupling constants [δ_H 3.24 (1H, dd, $J_{3,2\alpha} = 4.6$ Hz and $J_{3,2\beta} = 11.7$ Hz); δ_C 79.0 (d)]. The absolute configuration of C-22 in **1** was determined to be *R* because coupling constants were observed [δ_H 4.23 (1H, dd, $J_{22,20\beta} = 3.4$ Hz and $J_{22,23} = 7.0$ Hz); δ_C 74.5 (d)], and significant NOEs were shown from H-22 to H-16α; H-22 to H-24; H-22 to H-17α; from H-17α to Me-21. Other NOEs were shown from Me-19 to H-2β and Me-29, from H-5α to H-7α, from H-6β to Me-19 and Me-29, from H-7α to Me-30, from H-12α to Me-21 and Me-30, from H-11β to Me-18. Therefore, A, B and C rings in **1** have chair/twist, chair/twist and chair conformation (Fig. 1). The geometry of the C-23 and C-24 was established as C-23*E* because the coupling constants [δ_H 5.70 (1H, dd, $J_{23,24} = 16.1$ Hz and $J_{23,22} = 7.0$ Hz.); δ_C 129.4 (d): H-23] and [δ_H 5.78 (1H, d, $J_{24,23} = 16.1$ Hz; δ_C 135.9 (d): H-24) were observed. These data established that the structure of compound **1** as lanosta-8,23*E*-diene-3β,22*R*,25-triol (**1**).

The minor compound **2** had the molecular formula $C_{30}H_{48}O_3$ (M^+; *m/z* 456.3603) by HREIMS. The IR spectrum showed a hydroxyl group (ν_{max} 3447 cm^{-1}). The ^1H and ^{13}C NMR spectra (Table 3) resembled those of **1** except for H-7 (δ_H 5.49), H-11 (δ_H 5.31) in ^1H NMR spectrum and C-7 [δ_C 120.5 (d)], C-8 [δ_C 142.3 (s)], C-9 [δ_C 146.0 (s)], C-11 [δ_C 116.0 (d)] in ^{13}C NMR spectrum. The HMBC spectrum showed long-range correlation between Me-19 and C-9, between Me-30 and C-8, between H-11 and C-8 and C-13. However, the chemical shifts and coupling constants in side chain (C-20–C-27) exhibited good agreement in **1** and **2**. The configuration at C-22 in **2** was deduced from chemical shift and coupling constants [δ_H 4.25 (1H, dd, $J_{22,20} = 3.8$ Hz and $J_{22,23} = 6.8$ Hz); δ_C 74.4 (d)], and the geometry of the disubstituted double bond was determined as *E* by the chemical shift

Table 1
NMR spectral data of compound **1** in $CDCl_3$

Position	δ_H[a]	*J*/Hz	$^1H-^1H$ COSY	NOE	δ_C	HMBC (C)[b]
1α	1.23 m		1β, 2α, 2β	1β, 2α, 3, 5, 11, 28	35.5 (t)	2, 3, 10, 19
1β	1.74 m		1α, 2α, 2β	1α, 11, 19		
2α	1.66 m		1α, 1β, 2β, 3	1α, 3	27.8 (t)	1, 3, 4, 10
2β	1.57 m		1α, 1β, 2α, 3	19, 29		
3	3.24 dd	11.7 (2β), 4.6 (2α)	2α, 2β	1α, 2α, 5, 28	79.0 (d)	1, 4, 28, 29
4					38.9 (s)	
5	1.05 dd	12.6 (6β), 2.1 (6α)	6α, 6β	1α, 3, 6α, 7, 30	50.3 (d)	1, 3, 6, 7, 9, 10, 19, 28, 29
6α	1.69 m		5, 6β, 7	5, 6β, 7, 28, 30	18.2 (t)	5, 7, 8, 10
6β	1.51 m		5, 6α, 7	6α, 7, 19, 29		
7	2.04 (2H, m)		6α, 6β	5, 6α, 6β, 15, 30	26.5 (t)	6, 8, 9
8					134.1 (s)	
9					134.6 (s)	
10					37.0	
11	2.02 (2H, m)		12	1α, 1β, 12, 18, 19	20.9 (t)	8, 9, 12
12	1.67 (2H, m)		11	11, 17, 18, 21, 30	30.9 (t)	9, 11, 13, 14, 18
13					44.7 (s)	
14					49.4 (s)	
15	1.20 (2H, m)		16α, 16β	7, 16α, 30	30.9 (t)	13, 14, 30
16α	1.89 m		15, 16β, 17	15, 16β, 17, 22, 24, 30	27.4 (t)	13, 15, 17, 20
16β	1.43 m		15, 16α, 17	16α, 18, 20, 22, 23		
17	1.43 m		16α, 16β, 20	12, 16α, 21, 22, 30	47.4 (d)	12, 13, 14, 15, 18, 20, 21, 22
18	0.73 s			11, 12, 16β, 19, 20, 21	15.9 (q)	12, 13, 14, 17
19	0.98 s			1β, 2β, 6β, 11, 18, 29	19.1 (q)	1, 5, 9, 10
20	1.79 m		17, 22	16β, 18, 21, 22	42.6 (d)	17, 22
21	0.93 d	6.7 (20)	20	12, 17, 18, 20, 23	12.6 (q)	17, 20, 22
22	4.23 dd	3.4 (20), 7.0 (23)	20, 23	16α, 16β, 17, 20, 23, 24	74.5 (d)	20, 21, 23, 24
23	5.70 dd	7.0 (22), 16.1 (24)	22, 24	16β, 21, 22, 27	129.4 (d)	22, 24, 25
24	5.78 d	16.1 (23)	23	16α, 22, 26	135.9 (d)	22, 23, 25, 26, 27
25					82.0 (s)	
26	1.35 s			24, 27	24.3 (q)	24, 25, 27
27	1.36 s			23, 26	24.5 (q)	24, 25, 26
28	1.00 s			1α, 3, 6α	27.9 (q)	3, 4, 5, 29
29	0.81 s			2β, 6β, 19	15.4 (q)	3, 4, 5, 28
30	0.83 s			5, 6α, 7, 12, 15, 16α, 17	24.1 (q)	8, 13, 14, 15

[a] ^1H chemical shift value (δ ppm from $SiMe_4$) followed by multiplicity and then the coupling constants (*J*/Hz). Figures in parentheses indicate the proton coupling with that position.
[b] Long-range $^1H-^{13}C$ correlations from H to C observed in the HMBC experiments.

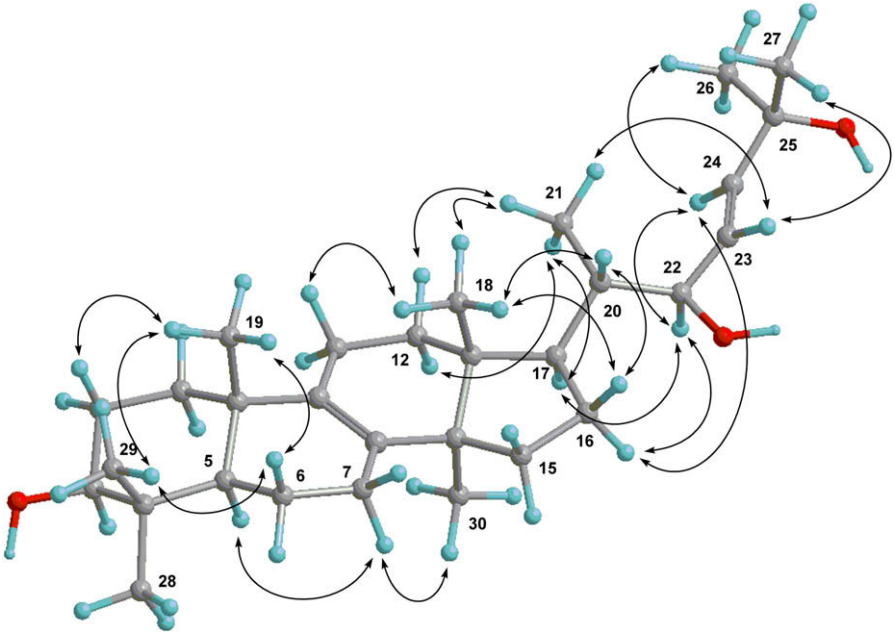

Fig. 1. Key NOE correlations for **1**.

and coupling constants [δ_H 5.73 (1H, dd, $J_{23,22} = 6.8$ Hz and $J_{23,24} = 16.0$ Hz.); δ_C 129.4 (d): H-23] and [δ_H 5.81 (1H, d, $J_{24,23} = 16.0$ Hz; δ_C 135.8 (d): H-24). The observed NOEs (Fig. 2) from Me-18/H-20; Me-21/Me-12β and H-17α; H-17α/H-22; H-22/H-24; Me-21/H-23 showed *R* configuration at C-22 and geometry at C-23 was *E*, which is same as those of **1**. Other NOEs were shown from H-7/Me-30, from H-11/H-1β. These data established the structure of compound **2** as lanosta-7:9(11),23*E*-triene-3β,22*R*,25-triol (**2**).

2.2. Biological evaluation

When Epstein-Barr virus (EBV–EA) is activated by tumor promoters, produces viral early antigens (EA), and the evaluation of their inhibitors is used as a primary screening for in vivo anti-tumor promoting activities [13].

Compounds **1**–**4** isolated from the sclerotia of *I. obliquus* were assayed for in vitro inhibitory activity against EBV–EA activation induced by TPA. All compounds exhibited dose-dependent inhibitory activities, and the viability percentages of Raji cells treated with the test compounds (**1**–**4**) were 70% at the highest concentration of 1000 mol ratio/TPA, suggesting that the cytotoxities of all compounds were moderate against in vitro cell lines (Table 2). As shown in Table 2, the inhibitory activities of compounds **1** ($IC_{50} = 231$), **2** ($IC_{50} = 228$), and **4** ($IC_{50} = 232$) except for compound **3** ($IC_{50} = 392$) were stronger at every concentration than that of oleanolic acid ($IC_{50} = 389$), known as a representative anti-tumor promoting agent [14]. The relative ratios of compound **2** with respect to TPA (100%) were 0, 25.1, 67.3 and 88.2% at the concentrations of 1000, 500, 100 and 10 mol ratio/TPA, respectively (Table 2); meaning 100, 74.9, 22.7 and 11.8% inhibition of the EBV–EA activation by TPA, respectively. Similarly, the relative ratios with respect to TPA (100%) were 0, 35.1, 64.0 and 90.4% for compound **4** at the concentrations of 1000, 500, 100 and 10 mol ratio/TPA, respectively (Table 2); meaning 100, 64.9, 36.0 and 9.6% inhibition of the EBV–EA activation by TPA, respectively. The inhibitory activities of compound **3** were weaker (10.9% at the concentration of 1000 mol ratio/TPA) as compared with those of compounds **1**, **2** and **4**. In conclusion, in studies on the inhibitory effects on EBV–EA activation of four lanostane-type triterpenoids, compounds **1**, **2** and **4** displayed their potent activities. It is interesting to note that 22,25-dihydroxy-23-ene or C-21 aldehyde group in lanostane-type triterpenoids are important to enhance the activity expression.

From this in vitro experiments and considering the yield we selected 3β-hydroxylanosta-8,24-dien-21-al (**4**) to examine the effect on the in vivo two-stage mouse-skin carcinogenesis with DMBA (390 nmol) and TPA (1.7 nmol, twice/week). After 20 weeks of promotion, there was no statistically significant difference in body weights between the control and the treated group. The activities were estimated by both the incidence (percentage of mice bearing papillomas, Fig. 3A) and the multiplicity (average number of papillomas, Fig. 3B). In the control group 100% of the mice bore papillomas of promotion (Fig. 3A), and 4.2 papillomas per mouse were formed at week 11. The tested compound **4** was able to inhibit the tumor promotion, reducing the percentage of mice bearing papillomas. In fact 33.3% of mice of the treated group bore papillomas, and developed 1.2 papillomas per mouse at week 11, and 73.3% and 3.8 papillomas ($P > 0.05$) at week 20 (Fig. 3A and B). This in vivo result showed that the inhibitory activity of compound **4** was stronger than that of oleanolic acid, the positive control or inotodiol, a main constituent from this sclerotia [10].

Compound **4** is related the most abundant triterpene, trametenolic acid [10], which constitutes above 15% of the extract from the sclerotia of *I. obliquus*, therefore, **4** can be supplied in a large amount. *I. obliquus* is harvested for daily use in many countries including Japan and it is used widely in Russia in particular. We plan to review structure–activity relationship of 21-substituted-lanost-8-ene analogs, and expect further investigation of *I. obliquus* will contribute to the society.

3. Experimental protocols

3.1. Chemistry

3.1.1. General

Melting points were determined on a Yanagimoto micro-melting point apparatus and are uncorrected. Optical rotations were measured using a JASCO DIP-1000 digital polarimeter. IR spectra were recorded using a Perkin–Elmer 1720X FTIR spectrophotometer. ^1H and ^{13}C NMR spectra were obtained on a Varian INOVA 500 spectrometer with standard pulse sequences, operating 500 and 125 MHz, respectively. $CDCl_3$ was used as the solvent and TMS as the internal standard. EIMS were recorded on a Hitachi 4000H double-focusing mass spectrometer (70 eV). Column chromatography was carried out over silica gel (70–230 mesh, Merck) and medium-pressure liquid chromatography (MPLC) was carried out with silica gel (230–400 mesh, Merck). HPLC was run on a JASCO PU-1586 instrument equipped with a differential refractometer (RI 1531). Fractions obtained from column chromatography were monitored by TLC (silica gel 60 F_{254}, Merck). Preparative TLC was carried out on Merck silica gel F_{254} plates (20 × 20 cm, 0.5 mm thick).

3.1.2. Material

I. obliquus (pers. Fr.) Pil. is succeeded in culture in Salad Melon Co Ltd., Nayoro City, Hokkaido, Japan. Sclerotium (4 kg) of *I. obliquus* was obtained from the above office at April, 2005.

3.1.3. Extraction and isolation

The sclerotia of white-rot fungus, *I. obliquus* (pers. Fr.) Pil. (4 kg) was extracted with $CHCl_3$ (10 L) employing an automatic percolator for 20 days at 60 °C. The $CHCl_3$ solution was evaporated under reduced pressure, and the resulting dark brown residue (153.9 g) was subjected to silica gel (3 kg) column chromatography. Elution of the column with $CHCl_3$/EtOAc (20:1) afforded residues A (Fr. No. 1–17,

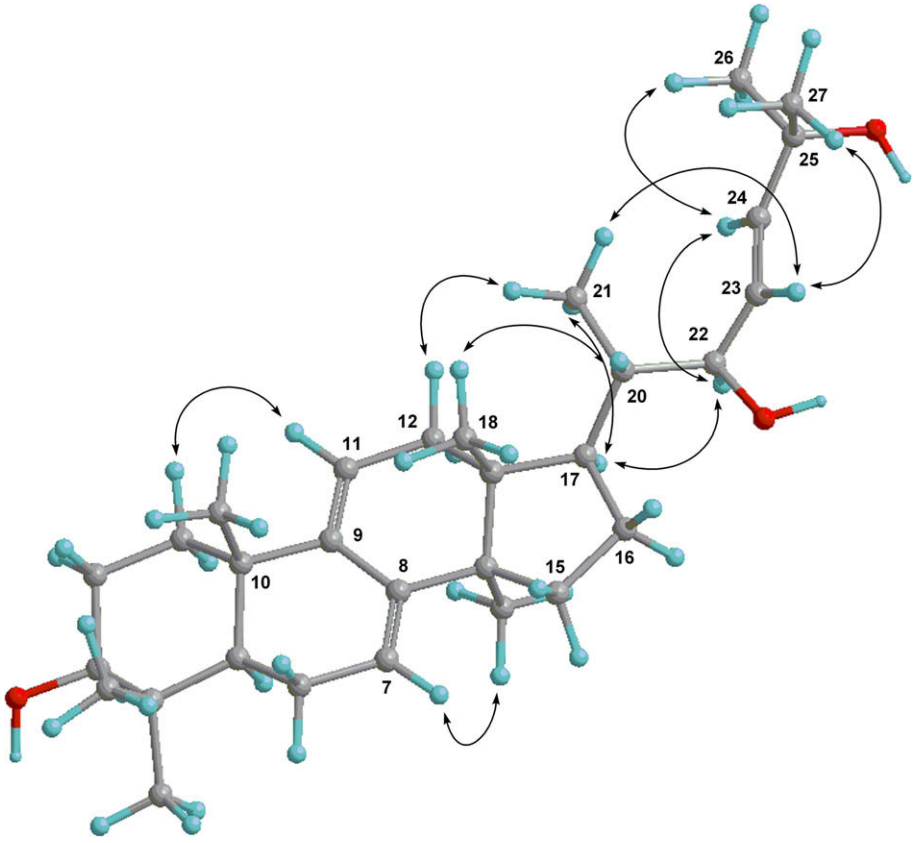

Fig. 2. Key NOE correlations for **2**.

4.9 g), B (Fr. No. 18–32, 23.6 g) and C (Fr. No. 33–51, 10.9 g). Elution was continued with $CHCl_3$/EtOAc (5:1) to give residue D (Fr. No. 52–87, 34.7 g) and subsequent column chromatography with $CHCl_3$/EtOAc (2:1) to give residue E (Fr. No. 88–120, 24.5 g), respectively. Residue B was rechromatographed over silica gel (70–230 mesh, 700 g) column chromatography using $CHCl_3$/EtOAc (10:1) to give residue B1 (Fr. No. 17–25, 5.93 g) and residue B2 (Fr. No. 26–29, 1.08 g). Residue B1 was rechromatographed on MPLC (230–400 mesh silica gel, 100 g) using *n*-hexane/EtOAc (4:1) to give a crystalline solid (Fr. No. 29–46, 3.78 g), which was recrystallized from MeOH/$CHCl_3$ to give compound **4** (2.68 g). Residue B2 was rechromatographed on MPLC (230–400 mesh silica gel, 50 g) using *n*-hexane/EtOAc (3:1) to give an amorphous solid (Fr. No. 46–55, 65 mg) which was separated with HPLC (ODS, 90% MeOH) to give compounds **1** (6.6 mg) and **2** (2.5 mg). Residue C was rechromatographed over silica gel (70–230 mesh, 700 g) column chromatography using $CHCl_3$/EtOAc (10:1) to give a crystalline solid (Fr. No. 48–58, 2.05 g), which was recrystallized from MeOH/$CHCl_3$ to give compound **3** (1.52 g). Compounds **3** and **4** were identified by already published data, and the chemical structures and the results of in vitro EBV–EA activation test are shown in Table 2. Compounds **1**–**4** had the purity of over 99.5%.

Table 2
Relative ratio[a] of EBV–EA activation with respect to positive control (100%) in the presence of **1**–**4** and oleanolic acid

Compounds	% to control (% viability)				IC_{50} (mol ratio/32 pmol/TPA)
	Concentration (mol ratio/TPA)[b]				
	1000	500	100	10	
1	0 (70)	26.9	69.8	89.2	231
2	0 (70)	25.1	67.3	88.2	228
3	10.9 (70)	47.1	77.5	100	392
4	0 (70)	35.1	64.0	90.4	232
Oleanolic acid	12.7 (70)	30.0	80.0	100	389

Values in parentheses are the viability percentages of Raji cells.
[a] Values represent percentages relative to the positive control value (100%).
[b] TPA concentration was 20 ng/ml (32 pmol/ml).

*3.1.3.1. Lanosta-8,23E-diene-3β,22R,25-triol (**1**).* Colourless crystals; mp 143–145 °C (from MeOH/$CHCl_3$); $[\alpha]_D^{16}$ 34.5° (*c* 0.72, $CHCl_3$); HREIMS *m/z*: 458.3759 $[M]^+$ ($C_{30}H_{50}O_3$, calcd for 458.3764); IR (KBr) ν_{max} cm^{-1}: 3447 (OH), 2966, 1457, 1374, 1287, 1028; ^1H and ^{13}C NMR, see Table 1. EIMS *m/z* (rel. int.): 458 (38) $[M]^+$, 440 (58) $[M-H_2O]^+$, 398 (43), 383 (53), 365 (43), 325 (36).

*3.1.3.2. Lanosta-7:9(11),23E-triene-3β,22R,25-triol (**2**).* Colourless crystal; $[\alpha]_D^{21}$ 157.8° (*c* 0.047, $CHCl_3$); HREIMS *m/z*: 456.3603 $[M]^+$ ($C_{30}H_{48}O_3$, calcd for 456.3603); IR (KBr) ν_{max} cm^{-1}: 3447 (OH), 2943, 1653, 1559, 1457, 1374, 1286, 1028, 753; ^1H and ^{13}C NMR, see Table 3. EIMS *m/z* (rel.

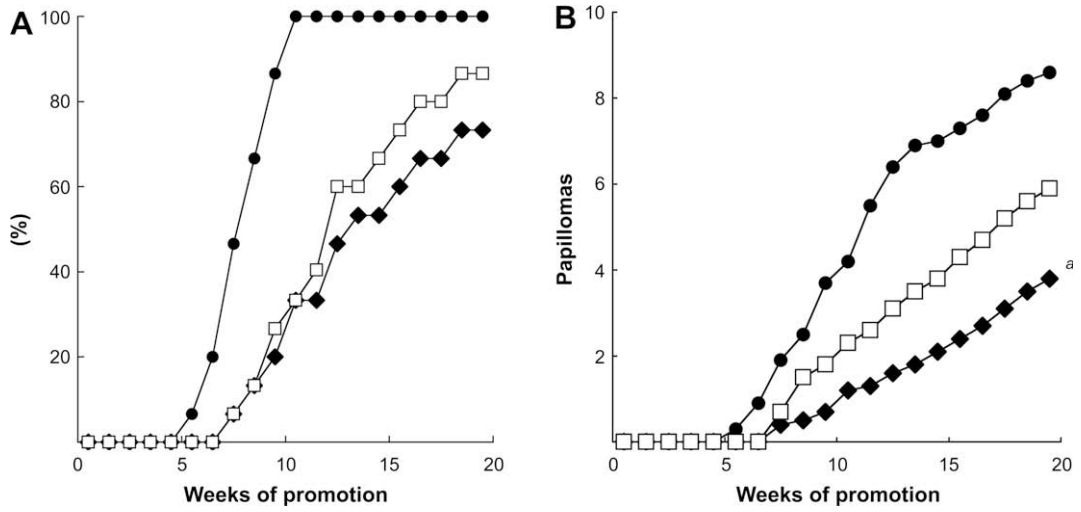

Fig. 3. Inhibition effects of 3β-hydroxylanosta-8,24-dien-21-al (**4**) on DMBA/TPA mouse-skin carcinogenesis. Tumor formation in all mice was initiated with DMBA (390 mmol) and promoted with TPA (1.7 nmol) twice weekly, starting 1 week after initiation. (A) Percentage of mice with papillomas. (B) Average number of papillomas/mouse. ● control (TPA alone); □ TPA + 85 nmol of positive control (oleanolic acid); ◆ TPA + 85 nmol of **4**. (*a*) Significantly different from positive control ($P < 0.05$).

Table 3
NMR spectral data of compound **2** in $CDCl_3$

Position	δ_H[a]	*J*/Hz	$^1H-^1H$ COSY	NOE	δ_C	HMBC (C)[b]
1	2.00 (2H, m)		2	2, 11, 19	35.7 (t)	2, 3, 5, 9, 10
2	1.70 (2H, m)		1, 3	1, 3, 19, 29	27.8 (t)	1, 4, 10
3	3.25 dd	11.4 (2β), 4.4 (2α)	2	2, 5, 28	78.9 (d)	1, 5, 28, 29
4					38.7 (s)	
5	1.13 m		6, 10	3, 6, 12α, 30	49.0 (d)	1, 3, 4, 9, 10, 19, 28, 29
6	2.09 m		5, 7	5, 7, 18, 19, 29	23.0 (t)	7, 8, 10
7	5.49 d	6.3 (6)	6	6, 15, 30	120.5 (d)	8, 9, 14
8					142.3 (s)	
9					146.0 (s)	
10					37.4 (s)	
11	5.31 d	6.0 (12)	12α, 12β	1, 12α, 12β, 19	116.0 (d)	8, 10, 13
12α	2.18 m		11, 12β	5, 11, 17, 21, 30	37.7 (t)	9, 11, 13, 14, 18
12β	2.08 m		11, 12α	11, 18, 21		
13					44.0 (s)	
14					49.9 (s)	
15	1.42 (2H, m)		16	7, 30	31.6 (t)	13, 17
16	2.04 (2H, m)		15, 17	18	26.5 (t)	13, 14, 20
17	1.49 m		16, 20	12α, 21, 22, 30	47.9 (d)	12, 14, 15, 18, 21, 22
18	0.60 s			6, 12β 16, 19, 20, 21	15.4 (q)	12, 13, 14, 17
19	0.98 s			1, 2, 6, 11, 18, 29	22.7 (q)	1, 5, 9, 10
20	1.80 m		17, 21, 22	18, 21, 22	42.4 (d)	22, 23
21	0.93 d	6.7 (20)	20	12α, 12β, 17, 18, 20, 23	12.4 (q)	17, 20, 22
22	4.25 dd	3.8 (20), 6.8 (23)	20, 23	17, 20, 23, 24	74.4 (d)	17, 20, 21, 23, 24
23	5.73 dd	6.8 (22), 16.0 (24)	22, 24	21, 22, 24, 26, 27	129.4 (d)	20, 22, 24, 25
24	5.81 dd	16.0 (23)	23	22, 23, 26, 27	135.8 (d)	22, 23, 25, 26, 27
25					82.1 (s)	
26	1.36 s			23, 24	24.4 (q)	24, 25, 27
27	1.37 s			23, 24	24.5 (q)	24, 25, 26
28	1.01 s			3, 30	28.0 (q)	3, 4, 5, 29
29	0.88 s			2, 6, 19	15.8 (q)	3, 4, 5, 28
30	0.83 s			5, 12α, 15, 17, 28	25.5 (q)	8, 13, 14, 15

[a] ^1H chemical shift value (δ ppm from $SiMe_4$) followed by multiplicity and then the coupling constants (*J*/Hz). Figures in parentheses indicate the proton coupling with that position.

[b] Long-range $^1H-^{13}C$ correlations from H to C observed in the HMBC experiments.

int.): 456 (22) $[M]^+$, 441 (20) $[M-Me]^+$, 438 (27) $[M-H_2O]^+$, 371 (21), 341 (58), 311 (66), 261 (36).

3.2. Bioassays

3.2.1. Inhibition of EBV–EA activation test

EBV–EA positive serum from a patient with nasopharyngeal carcinoma (NPC) was a gift from the Department of Biochemistry, Oita Medicinal University. The EBV genome-carrying lymphoblastoid cells (Raji cells derived from Burkitts lymphoma) were cultured in 10% fetal bovine serum (FBS) in RPMI-1640 medium (Nissui). Spontaneous activation of EBV–EA in our sub-line Raji cells was less than 0.1%. The inhibition of EBV–EA activation was assayed using Raji cells (virus non-producer type) as described previously [13]. The indicator cells (Raji cells, 1×10^6/ml) were incubated at 37 °C for 48 h in 1 ml of a medium containing *n*-butyric acid (4 mmol), TPA (32 pmol = 20 ng in dimethylsulfoxide (DMSO), 2 μl) as inducer and various amounts of test compounds in 5 μl DMSO. Smears were made from the cell suspension, and the activated cells that were stained by EBV–EA positive serum from NPC patients were detected by an indirect immunofluorescence technique [5]. In each assay, at least 500 cells were counted, and the number of stained cells (positive cells) present was recorded. Triplicate assays were performed for each compound. The average EBV–EA induction of the test compounds was expressed as a relative ratio to the control experiment (100%) which was carried out only with *n*-butylic acid (4 mmol) plus TPA (32 pmol). EBV–EA induction was ordinarily around 35%. The viability of treated Raji cells was assayed by the Trypan Blue staining method.

3.2.2. Two-stage mouse-skin carcinogenesis test

Mouse studies were approved by the committee of Animal Experimental Center for Kyoto Prefectural University of Medicine throughout all treatments. Non-infective mice (SENCAR mice) (6 weeks old) were obtained from Japan SLC Inc., Shizuoka, Japan, and the animals were housed, five per polycarbonate cage, in a temperature-controlled room at 24 °C and given food and water ad libitum throughout the experiment. Animals were divided into three experimental groups containing 15 mice each. The back of each mouse was shaved with surgical clippers, and the mice were topically treated with DMBA (100 ng, 390 nmol) in acetone (0.1 ml) as an initiating treatment. One week after the initiation, papilloma formation was promoted twice weekly by the application of TPA (1 ng, 1.7 nmol) in acetone (0.1 ml) to the skin. One hour before each treatment, the mice were treated with the samples (85 nmol) in acetone (0.1 ml). The incidence of papillomas was examined weekly over a period of 20 weeks. Student's *t* test was used for all statistical analysis.

Acknowledgements

This study was supported by a Grant-Aid High Technology from the Ministry of Educations, Sports and Culture, Japan.

References

[1] M.B. Sporn, Cancer Res. 59 (1999) 4743.
[2] W.K. Hong, M.B. Sporn, Science 278 (1997) 1073.
[3] I. Berenblum, Cancer Res. 1 (1941) 807.
[4] M.H.D. Postema, J.L. Piper, R.L. Betts, F.A. Valeriote, H. Pietraskewicz, J. Org. Chem. 70 (2005) 829.
[5] R. Tanaka, T. Minami, K. Tsujimoto, S. Matsunaga, H. Tokuda, H. Nishino, Y. Terada, A. Yoshitake, Cancer Lett. 172 (2001) 119.
[6] D.L. Hawksworth, P.M. Kirk, B.C. Sutton, D.N. Pegler, Ainsworth and Bisbi's Dictionary of the Fungi CAB International, eighth ed.). University Press, Cambridge, 1995, p. 616.
[7] M.B. Ellis, P.J. Ellis, Fungi Without Gills (Hymenomycetes and Gasteromycetes): An Identification Handbook, Chapman and Hall, London, 1990, p. 329.
[8] Y.M. Park, J.H. Won, Y.H. Kim, J.W. Choj, H.J. Park, K.T. Lee, J. Ethnopharmacol. 101 (2005) 120.
[9] K. Kahlos, L. Kangas, R. Hiltunen, Acta Pharm. Fennica 96 (1987) 33.
[10] T. Nakata, T. Yamada, S. Taji, H. Ohishi, S. Wada, H. Tokuda, K. Sakuma, R. Tanaka, Bioorg. Med. Chem. 15 (2007) 257.
[11] D.A. Benson, I. Karsch-Mizrachi, D.J. Lipman, J. Ostell, B.A. Rapp, D.L. Wheeler, GenBank. Nucl. Acids Res. 28 (2000) 18.
[12] K. Kahlos, R. Hiltunen, M. Von Schants, Planta Med. 50 (1984) 197.
[13] Y. Ito, M. Kawanishi, T. Harayama, S. Takabayashi, Cancer Lett. 12 (1981) 175.
[14] T. Konoshima, M. Takasaki, M. Kozuka, H. Tokuda, J. Nat. Prod. 50 (1987) 1167.